

## Calculations on different length scales for improving processing of nanoceramics

Wilfried Wunderlich\*

Nagoya Institute of Technology, Dept. of Environmental Technology, Gokiso, Showa-ku, 466-8555 Nagoya, Japan

Advanced processing of nano-ceramic composite materials requires an understanding of physical phenomena on an atomistic scale by *ab-initio* calculations. This overview continues a previous report and is divided into three parts. After describing the goals and the range of possible applications of such simulations, the needs for simulations of new applications of ceramics, namely for photovoltaic and thermoelectric materials, are briefly summarized. The most challenging subject for *ab-initio* calculations, however, is an understanding of physical phenomena in aqueous solutions and their present results are described in the third part. Based on experimental results, the simulation of Al-Mg-spinel formation with different methods, the discrete element method (DEM) and Molecular Dynamics (MD) is described. The appropriate approach for the numerical treatment of these many-particle interactions in liquids is the Voronoi- method, for which some new ideas are presented in this paper. For *ab-initio* calculations the software Vasp with its great facilities is appropriate.

**Key words:** Sol-Gel process, Nano-ceramics, Al-Mg-Spinel, Discrete element method, Modeling of slurry phenomena, Voronoi diagram, Electron dispersion relation, Thermoelectric materials.

### Introduction

Processing of nano-ceramic composite materials is a challenge for the present age of materials science. Compared to conventional materials the processing techniques for nano-ceramics are more complicated, since the nano-crystallites are less stable and tend to collapse to larger agglomerates. This report is a continuation of a similar overview published recently [1], which showed examples of ceramic nano-particles and interface calculations. The present paper shows calculations of ceramic nano-particles on different length scales. Furthermore, the theory of electronic calculations and band structure calculations are described for reaching the goal, to develop new materials or improve materials processing by meaningful simulations. This overview paper can only give some outlines, since this subject covers a huge area and is still developing very rapidly.

The paper is divided into three parts: After describing the needs for the simulation of nano-ceramics, simulations of species in aqueous solutions and nano-particles, the geometry of simulations, the calculation methods, and the physical meaning of simulations are outlined.

### Needs for Simulation

#### Material development

The needs for *ab-initio*- and simulations on an atomic scale (Fig. 1) can be divided into screening,

microstructure improvement, analyzing new physical effects and process modeling. The screening focuses on the search for new material compositions, composite materials [2], or special geometries such as in gradient materials. Expensive experiments with e.g. specimens containing rare earth or the analysis of hydrogen, require simulations, which are relatively cheap. The microstructure of devices can be improved with the aid of simulations, to find optimal particle coatings or thin film microstructures. The influence of segregation, grain boundary or interfacial structures [3], vacancies, or interstitials can be calculated in the computer more easily compared to time-consuming experiments. New physical effects have been found by *ab-initio* calculations, like nano-size effects in ceramic particles, electron excitation effects, electron coupling etc., and also their understanding can be improved by simulation, in order to find better thermoelectric materials, electro-ceramics, photovoltaic materials, or precursor materials. For research in ceramics engineering, calculations can support the understanding of occurring phenomena in chemistry, physics or engineering, and problems are much easier to solve, when the reason can be found. Finally, for ceramics processing the understanding and data about the chemical reactions, like reaction probability, reaction path or sequence of the reactants or reaction velocities are essential. When using polymers the understanding of bonding to the inorganic surface is important. When applying the material for photo-catalysis, photochemistry, or photovoltaic cells, an understanding of the photon excitement by simulation is essential, as described in the next section. Finally, for an understanding of phenomena occurring during processing, like slip-casting, the adhesion of particles etc. simulations are necessary

\*Corresponding author:  
Tel : +81-90-7436-0253  
Fax: +81-52-735-5379  
E-mail: wunder@system.nitech.ac.jp

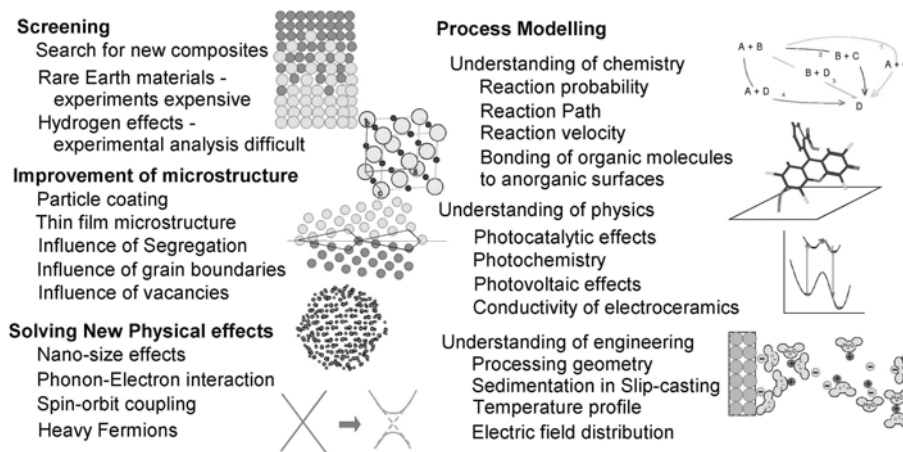


**Fig. 1.** Needs for atomistic and *ab-initio*- calculations in nano-ceramics processing.

as described in section 3.

### Photochemical reaction

Excitation of electrons by photons can be used for advanced material processing by photochemistry, for photovoltaic cells, or photo-catalytic reactions and the first two are described briefly. The use of light for material processing is able to produce sub-micrometer fine structures [4], because the place of the photochemical reaction can be controlled precisely. During this microstructural patterning a chemical reaction at the organic silica-precursor is enhanced by light, which transforms the surface to hydrophilic bonds, and only there are suitable molecules able to bond with the  $\text{TiO}_2$  particles are able to bond. After precursor burn-out and sintering the sub-micro structured ceramic is achieved.

Wet regenerative photo-electrochemical cells, the so-called Graetzel cells, can convert light into electricity with an efficiency better than 10%. The principle is the photo-induced charge separation based on the electron injection by visible light by an absorbing dye into a non-absorbing wide bandgap semiconductor such as  $\text{TiO}_2$  or  $\text{ZnO}$ . These so-called dye-sensitization solar cells could be improved [5] by the use of a highly porous thin film processed by sintering of nano-sized semiconductor particles, because dye-sensitization occurs only, when the dye molecules are directly bonded to the semiconductor surface as a quasi-monolayer. The three-dimensional enlargement of the active semiconductor/dye interface has achieved effective photon harvesting and high light-to-electric conversion efficiency, because the processing and the characterization of the photochemical properties of the semiconductor/dye hybrid material have been improved [5-7]. Simulation on atomic scale are needed in order to improve the processing as described in section 3 and to understand the excitation and decay of the photons and their kinetics [7] across the organic/anorganic interface in this system, as described in the previous paper [1]. These relatively cheap solar-cells and the following

thermoelectric materials considered can help to improve the energy supply in the future.

### Thermoelectric materials

The second challenging field of ceramics development considered here is the improving of thermoelectric materials. After the discovery of the high Seebeck-coefficient in  $\text{NaCoO}_4$  [8] this material is considered as a part of a suitable thermoelectric device for converting e.g. waste heat into electricity. The explanation of the physical reason for the unusual high positive thermo-power is still a challenge [9-11]. This material consists of strongly correlated conducting layers of  $\text{CoO}_4$  tetrahedrons and a disordered insulating layer. Research results showed that the conventional one electron picture, on which common band calculations are based, fails [12], but instead strong electron-electron correlation, called heavy-fermion coupling, plays an important role in the enhancement of the thermo-power [9-10]. The present model is that the heavy-fermion coupling in the strongly correlated layer increases the thermo-power through the mass enhancement due to spin fluctuation. The low-spin state of  $\text{Co}^{3+}$  sites in  $\text{NaCo}_2\text{O}_4$  is the main reason for the large thermo-power and both, the large degeneracies in the  $\text{Co}^{3+}$  and  $\text{Co}^{4+}$  sites, and the ratio between them is important for the enhancement of thermo-power [11]. In other heavy-fermion systems the Fermi surface and the effective mass have been measured by the de Haas-van Alphen experiment and the results were compared with enhanced band structure calculation based on the plane-wave-method [13], which shows that the developing of calculation methods for understanding these coupling effects is progressing.

Efficient thermo-power materials should possess a poor thermal conductivity and a high electric conductivity, which can be achieved e.g. by ions weakly bound in an oversized atomic cage so that they can vibrate independently from the other atoms [9], realized in the so-called clathrate crystals, like e.g.  $\text{Eu}_8\text{Ga}_{16}\text{Ge}_{30}$  [14-16]. The vibration in their atomic cage, which are

called “rattling” or “rattling site”, leads to a very short phonon mean free path, almost as short as the lattice parameters, and hence much shorter than the electron mean free path. This is the reason for the poor thermal conduction of this material like a glass and for the good electric conduction like a crystal, and therefore these materials are called “a phonon glass and an electron crystal”. Also  $\text{NaCo}_2\text{O}_4$  shows the properties like a phonon glass- electron crystal- material, however, the reason is still unclear, since it has no rattling sites [9].

Thermoelectric devices consist of two types of materials, one with positive, and the other with negative thermo-power.  $\text{NaCo}_2\text{O}_4$  belongs to the first type and the search for the second type is also progressing, since conventional n-doped semiconductors are not sufficient. Also clathrate materials have a high negative thermo-power and the required low thermal conductivity, but the electrical resistance needs to be improved [14-16].

After this excursion into this new subject of material physics, which still need the development of theories or appropriate software, material science problems are described in the following text, which can be simulated by presently available software.

## Experiment and calculation of nano-particles

### Example of $\text{Al}_2\text{O}_3$ -MgO nano-composite

In the following the simulation of ceramic slurries in different length scales is described. In most of the cases the motivation for modeling and calculation comes from experiments. A typical example for low-cost production of nano-ceramics is the sol-gel method, for which a typical flowchart is shown in Fig. 2 for the example of an alumina-magnesia nano-composite ceramic [17]. This polymeric sol-gel route was also modified by changing the type of salt, and other composites, like  $\text{Al}_2\text{O}_3$ -Ag [18, 19],  $\text{Al}_2\text{O}_3$ - $\text{TiO}_2$  [20],  $\text{Al}_2\text{O}_3$ - $\text{SiO}_2$  [21],  $\text{Al}_2\text{O}_3$ - $\text{ZrO}_2$  (ZTA) [22] could successfully be manufactured. Differential thermal analysis (DTA), thermal gravity (TG) and differential thermal gravity (DTG) clarified, which species are present in this aqueous solution during each process step (Fig. 2). The precursor aluminium-isopropoxide was hydrolyzed for 80 min and transformed into Boehemite by releasing Propyl-alcohol. Then the magnesia-nitrate salt was added and mixed with nitric acid for peptization, which was carried out also for 80 min. This sol precipitated as boehmite in an ammonia solution after ageing for 12h. This gel was filtered and dried at  $120^\circ\text{C}$  for 6h. After drying an amorphous alumina-magnesia composite is formed, which transforms during firing via  $\alpha$ -alumina and brucite, to Al-Mg-spinel as confirmed by TEM observations.

These experimental results were compared with thermodynamic calculations by summing up the Gibbs free enthalpies and their temperature dependence for the three reactions [17], which are likely to occur in the

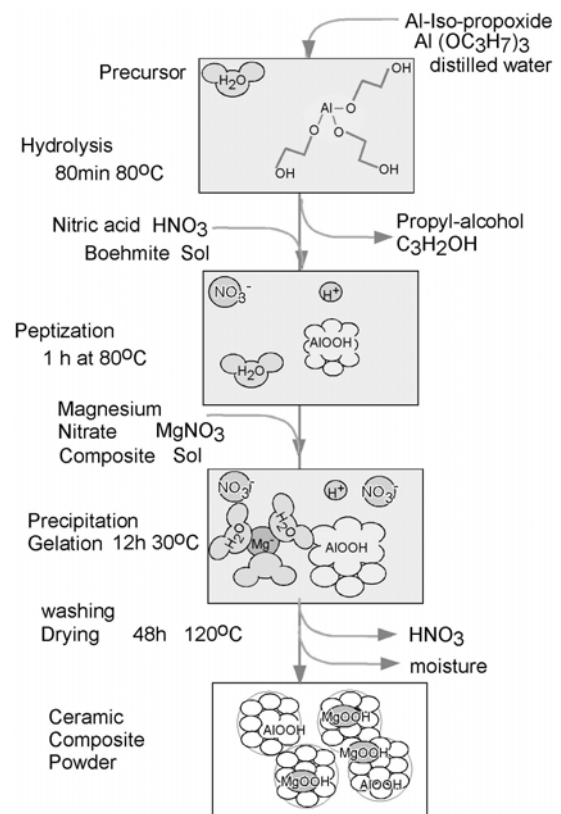


Fig. 2. Flowchart of a typical sol-gel processing route, in this example  $\text{Al}_2\text{O}_3$ -MgO-nano-composite, showing the species in aqueous solution.

slurry, namely the hydrolysis reaction of alumina and magnesia and the spinel formation. Both, experiments and calculation agree well with the phase diagram published for this reaction. This example showed, that the reaction path could be experimentally determined by the conventional combination of DTA, DTG, TEM. MD- calculations reported in section 3.3 showed that for nano- particles special size effects occur, so that the phase diagram has to be revised. Hence, for nano-ceramics new characterization methods are required, for example, electrical conductivity measurements [22] during heating a Si-O-C precursor composite could characterize their transformation behavior into ceramics.

Optimization of ceramic processing requires a balance between attractive and repulsive forces between the particles. Illustrations like Fig. 3 help, to distinguish the different types of slurry stabilization [23-25]. With steric stabilization long polymer chains maintain a distance between the ceramic particles. When the polymer molecules are not bond to the particles, a repulsion by depletion occurs. The most effective repulsion is performed by Coulomb forces caused by polarization of the particle surface either in the acid or base region left or right of the iso-electric point. This electrostatic repulsion can be performed by ions or charged polymer chains or both.

On an atomic scale the charge distribution on particle

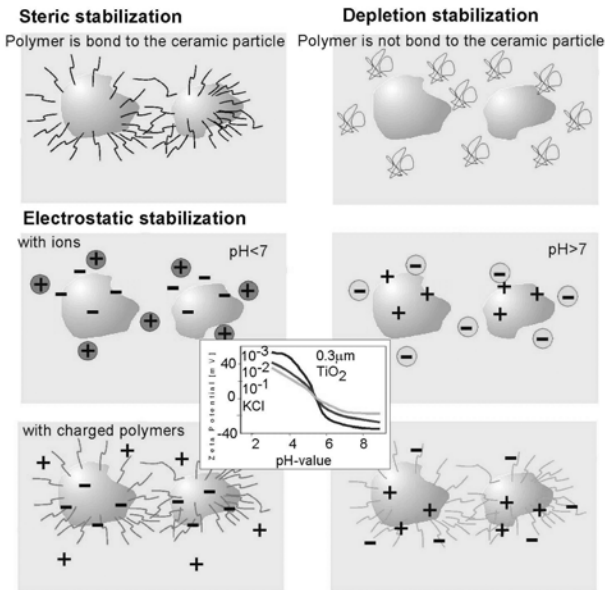


Fig. 3. Interaction forces between species in aqueous solutions.

surfaces has been explained by the so-called DLVO model named after the scientists B.V. Derjaguin, L.D. Landau, E.J.W. Verwey, J.T.G. Overbeck [23, 24]. Figure 4 shows the case, that cations have a higher absorption ratio to the ceramic surface, so that a negative charge at the surface is formed. Hence, the probability is high, that in the next layer of molecules between the inner and outer Helmholtz layer (IHP, OHP) positive charged particles are in the majority. In the subsequent layer, so-called stern-layer, the potential reaches the level of the aqueous solution. In the case, that anions have a higher absorption rate, the IHP and OHP have opposite charge. For quantitative understanding of these phenomena simulation is necessary.

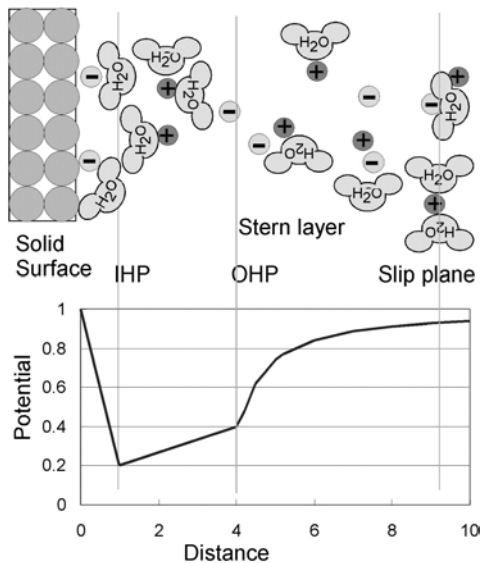


Fig. 4. Detail on atomistic scale of the electric potential at the particle surface.

Modeling of aqueous solutions by DEM

The so called Discrete Element Method (DEM) [28, 29] is a simulation method on a mesoscopic scale, which treats the interactions in the slurry between ceramic particles by semi-empirical parameters. The superposition of the attractive Van-der Waals (VdW)-term and the repulsive term leads to the DEM potential, which depends on the radii of the interacting particles  $r_1, r_2$ , their distances  $d$ , the Hamacker-constant of the liquid  $A_H$ , the Debye Hueckel-parameter  $k$ , and the pre-exponential term  $P$  in the repulsive term. The later two parameters  $k, P$  contain the dependence on the dielectric constant of the electrolyte  $\epsilon_r$ , its concentration  $c$  and valence  $Z$ , and the Zeta potential of the particles  $\Psi$ . Parameter sets for different powders in different liquids e.g.  $Al_2O_3$ ,  $t-ZrO_2$ ,  $BaTiO_3$  are available [28].

The following example for particles of  $Al_2O_3$ ,  $MgO$ , and  $MgAl_2O_4$  in air (Fig. 5a) [29] were calculated for  $r_1=r_2=100\text{ nm}$ ,  $[A_H=70 \cdot 10^{-20}\text{ J}, k=0.03 \cdot 10^{-7} \text{ 1/m}, P=50 \dots 400 \cdot 10^{-20}\text{ J}]$ . The energy increases, when the distance between particles is reduced because of long-range repulsive forces until a certain distance is reached, where agglomeration occurs. Using the same parameters for nano-particles ( $r_1=r_2=1\text{ nm}$ ) shows, that the repulsive forces almost disappeared (Fig. 5b). The data points correspond to MD-calculations for these particles.

The goal of ceramic processing is to achieve a perfect colloidal crystal by sufficiently strong repulsive forces, since agglomerations should be avoided. In the case of nano-particles this becomes difficult and strong repulsive forces can only be obtained, when the term containing the Debye-Hueckel-parameter  $k$  or the pre-exponential term  $P$  are increased by increasing the dielectric constant  $\epsilon_r$  of the liquid media, the Zeta Potential  $\Psi$  of the particles or the concentration of the electrolyte. The DEM simulation can support useful information not only for particle agglomeration as shown here, but also for sedimentation, centrifugation, slip casting etc., but for a deeper understanding at the

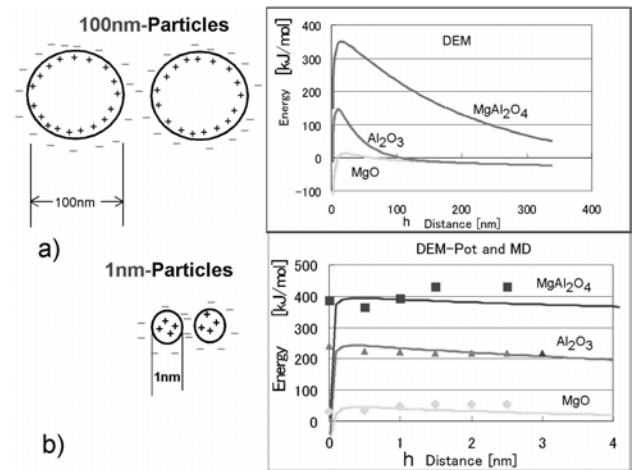


Fig. 5. Calculation of repulsive forces by discrete element method (DEM). (a) 100 nm, (b) 1 nm particles

atomistic level the following MD-simulations are necessary.

### Modeling of particle interactions by MD

In molecular dynamics (MD)-calculations the dynamic behavior of atoms is modeled by assuming a suitable interaction potential or force field between the atoms. A software program called Yasp [30, 31] is available, with which the dynamics and properties of polymers or other molecules in liquids can be simulated [30-32], but for its application the search of suitable MD-potentials is necessary, which can be difficult, because the potential parameters can depend on the liquid environment. For crystals, where the environment is almost unchanged, suitable parameter sets for the Buckingham/Morse potential for  $\text{Al}_2\text{O}_3$ , MgO and  $\text{MgAl}_2\text{O}_4$  can be found by fitting the parameters to macroscopic properties, like lattice constants, and thermal expansion coefficients from single crystal experiments [33]. The numerical MD-simulations for this paper on nano-particles were performed with the software called Moldy [34], which calculates the forces in reciprocal space and is especially suitable for ionic and covalent bonded materials. By normalizing the single crystal calculations according to the number of mols, the reaction enthalpy of each phase can be evaluated, which makes reliable, quantitative MD calculations of composite materials possible.

In composite materials the interfaces between materials can have different geometries. Figure 6 shows models on an atomic scale used for MD calculations in our laboratory. The planar interface e.g. between thin films of spinel on an alumina substrate (Fig. 6a) [35] is usually considered as the standard model for the interface energy. As can be seen from the atomic model, the oxygen sub-lattice is penetrating through the interface. For nano-particles the surface energy increased steeply as a function of the radius (Fig. 6b) [36] as described in the previous report [1], while for nano-pores it decreased (Fig. 6d) [36]. The same is expected for inter-nano-composites (Fig. 6d [37]). By approaching two nano-particles (Fig. 6b) [29] or at droplets on substrates (Fig. 6e) [38] the particles adjust their contact angle due to a balance between surface and interface energy even on nano-scale. Finally coated particles, like alumina coated with organic butane-chains (Fig. 6c), or particles encapsulated in nanotubes (Fig. 6g) reduce their energy by relaxing the atoms at interfaces.

By MD the interface and surface energies can be calculated with high accuracy [39] and it would be interesting to compare the influence of the geometry. The typical size for supercells in affordable MD calculations already exceeds 20000 atoms and hence, also mesoscopic effects can be calculated, like misfit dislocations, interaction of dislocations, particle interactions etc. However, the MD results strongly depend on the reliability of the potentials and their search can take a long time. Furthermore, it cannot be excluded, that the inter-atomic potentials will change at defects. That is

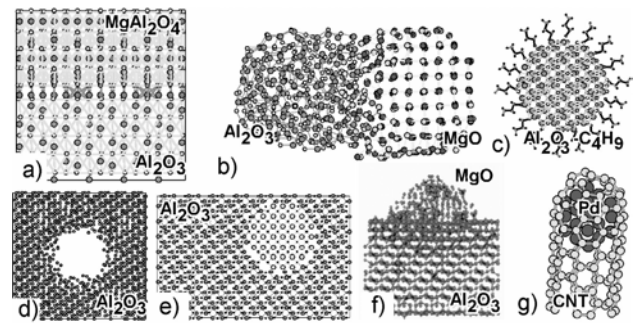


**Fig. 6.** Geometry of interfaces and nano-particles on atomic scale calculated by Molecular Dynamics, (a) planar, (b) between particles, (c) particle coating, (d) nano-pores, (e) inter-nano-composites, (f) nano-droplets (g) nano-particles encapsulated in nano-tubes.

the reason, why ab-initio methods are becoming more and more popular, although affordable calculations are restricted to about 100 atoms. They are described in section 3.5, but before that, a mathematical construction useful for both MD or *ab-initio* calculations is considered.

### Modeling of aqueous solutions by the Voronoi method

The following mathematical method is still under development and might in future be a promising tool to accelerate any particle calculation method, especially for treating particles or atoms in an amorphous environment like a liquid. The Voronoi construction is a numerical mathematical method for fast and effective characterizing of many microstructural properties [40] (Fig. 7), like the empty space between particles, the nearest neighbor distances, opens channels and their distribution, etc. The particles can be conventional ceramic particles on a macroscopic scale, nano-particles or atoms and can have the same radius (Fig. 7a), a bimodal distribution or a broad distribution of radii.

The construction can be performed mainly in two ways, usually referred as Voronoi- or Wigner-Seitz-method. In the first method, lines are drawn from the center of each particle to their nearest neighbors. These lines form polygons (Fig. 7b) or, in three-dimensions,

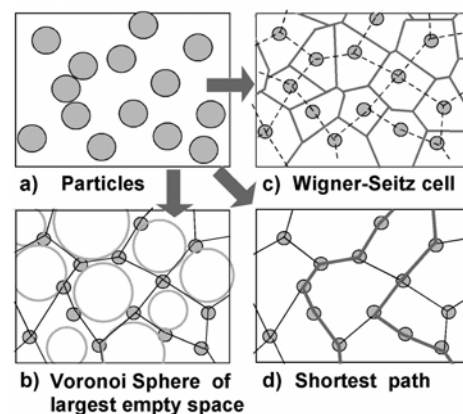


**Fig. 7.** Relationship between (a) particles, (b) Construction of Voronoi spheres, (c) Wigner-Seitz cells, (d) shortest path.

polyhedrons, which are equivalent to the Bernal polyhedrons describing e.g. the atomic arrangement in amorphous materials or liquids. The next step is to find the largest sphere inside these polyhedrons and their center defines the point set of the Voronoi diagram, which leads to further analysis of the microstructure, like the broadest path, largest empty space etc. [40]. The second method (Fig. 7c) is the Wigner-Seitz-cell construction, in which the shortest distance between the particles is divided into its half and the spatial distribution of the endpoints of all of these vectors leads to polyhedrons with their centers at the particle centers. This method is used for the construction of the Brillion Zone in reciprocal space. In the Wigner-Seitz construction the polyhedron is a measure of the environment affecting the particle, while in the Voronoi method the sphere describes the empty space between particles and it depends on the actual physical problem, which method is the more suitable one. A third analysis considers the shortest path between particles (Fig. 7d), which is important e.g. for the calculation of electric conductivity in composite materials of conducting and isolating particles.

The regular arrangement of equi-radii particles, e.g. atoms in closed packed crystals or particles in a colloidal crystal (Fig. 8a), leads to a regular pattern of the Voronoi spheres. Also, if diffraction in reciprocal space on these particles is considered, like electron diffraction at atoms or optical diffraction on colloidal particles, a regular point pattern with high symmetry is obtained. The Voronoi diagram of this pattern is the same as in case of hexagonal symmetry. In the case of *bcc* it transforms to *fcc* pattern and vice versa. Due to the high symmetry also equi-radii spheres are obtained.

The situation changes, if we now consider particles in a liquid (Fig. 8b). Even when the particles have the same radii, the Voronoi spheres have random sizes. The diffraction pattern in reciprocal (*k*-) space, e.g. obtained in the computer by fast Fourier transformation (FFT), shows a random distribution of diffraction spots in the outer regions, but a certain accumulation of spots in a

first and second ring near the center spot as described by the radial distribution function (RDF, inset in Fig. 8b). The reason for the RDF-shape with a clear first maximum, and dissipation for larger *k*-distances is the balance between adhesion and repulsive forces between the particles. The Voronoi construction of this diffraction pattern leads to polyhedrons with mostly elongated shapes containing large circles in their centers. Beyond the rim of the first maximum in the RDF the spheres become smaller and smaller, and the polyhedron sphere-like. It would be a challenge to find out, whether there is a simple transformation between the Voronoi sphere in real and reciprocal space and also how the corresponding Wigner-Seitz cells will transform.

The characterization of the microstructure by such mathematical methods is necessary to study the physical properties. The polyhedron in reciprocal space describes the scattering behavior of waves, and the schematic drawing (Fig. 8b) shows, that only the large polyhedrons near the center are significant for the physical properties of the material. Using the Voronoi construction in reciprocal space, physical effect for particles in liquids can be easily analyzed, like the Braggs law of scattering electromagnetic waves, the excitation of photons, or calculating the conductivity of electrolytes or amorphous materials. This Voronoi construction becomes dependant on the position, when the particle distribution is inhomogeneous, like at sedimentation or in the vicinity of electrodes. The application of this method will be progressing, when it can be adapted to common MD- or *ab-initio*- software packages.

### *Ab-initio* calculations

The most sophisticated and powerful calculation method for material science is the first-principle or *ab-initio*-method, which is based on the density functional theory (DFT) [41] and needs no empirical parameters. The many-body problem of calculating electrons in the Coulomb potential of the atom cores is simplified by assuming a single electron affected by a pseudo-potential, including the contributions of the atomic

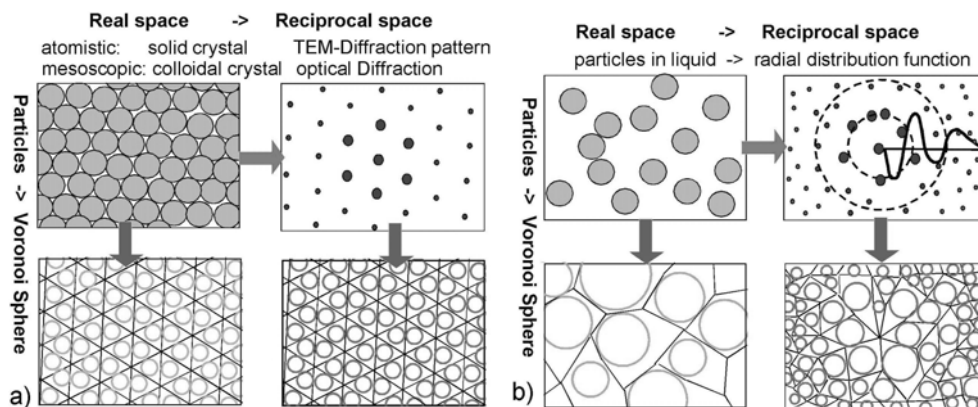


**Fig. 8.** Schematic drawing of the transformation from real space to reciprocal space, and the Voronoi construction, (a) for atoms in a crystal or for nano-particles on mesoscopic scale, (b) for diluted atoms or particles in aqueous solutions

core, the core electrons, and other electron wave functions. The theory was developed by starting from the three extreme cases, nearly free electrons, tight binding and electron levels at covalent bonds. The charge density is calculated self-consistently in the computer by an appropriate software program. Such a program is Vasp [41-45], which is well accepted in the community and widely used because of its reliability. It includes many facilities, like e.g. calculating the forces between atoms, which allows the atom migration into relaxed positions and make dynamic studies possible. Vasp has the advantage that it calculates absolute energy values, which only depend on the element and its input pseudo-potential [43]. Hence, the total energy output can be used directly for comparing different input structures and this is one of the ways to use electronic calculations as a vehicle for material science applications. In more sophisticated applications the density of states and the electron dispersion curve are calculated and interpreted as explained in the last chapter of this paper.

The application of the *ab-initio* program Vasp is straightforward: After creating the files with the atomic positions, the appropriate  $k$ -point settings, potentials and the control parameters, the self-consistent calculation starts. The density of states (DOS) as a function of the energy were calculated for a nickel oxide single crystal (Fig. 9) for different lattice constants as shown on the right ( $E(V)$ -calculations). The lowest energy was obtained for the underlined value of  $a=0.4051$  nm, which is in good agreement to the experimental value 0.4190 nm. The energy of the metallic Ni orbital decreases when increasing the lattice parameter, as observed in other two-atom materials, while the contribution of O orbitals are weak and affects only the fine structure of the DOS.

Many material science problems have successfully been calculated by Vasp: Adsorption of molecules on surfaces [46-48], transport properties in liquids [49], colors of intermetallics [50], etc. Also the electric conductivity of amorphous materials [51] has been calculated from first principles by splitting the band gap into gaps with different depths and widths. A

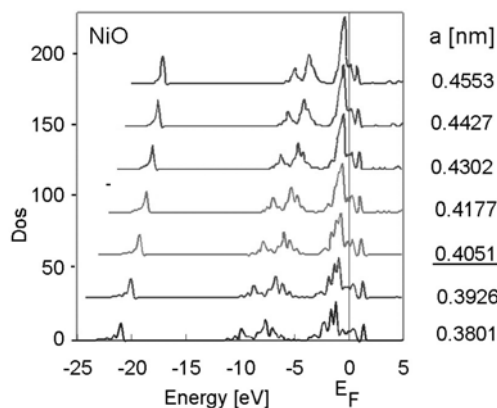


**Fig. 9.** Density of states for NiO by varying the lattice constant relative to the underlined bulk value.

Greens-function concept correlated this distribution with an average pseudo gap, and using the Kubo-Greenwood theory the calculated conductivity is in good agreement with the experimentally measured one. However, unrealistic scattered waves appeared due to a limited supercell, which had to be distinguished by artificial virtual sources or filtered out in reciprocal space and perhaps the promising Voronoi approach described in the previous section can simplify these calculations.

### Interpretation of Band structure calculations

By *ab-initio* calculations band structure diagrams are obtained, which need a proper interpretation in order to understand and optimize optical and electrical properties of materials. Figure 10 shows typical features occurring in such energy dispersion curves in reciprocal space ( $k$ -space) as deduced from textbooks [52-54]. The Fermi-Energy is marked as a dashed line and the band width or overlap between bands (Fig. 10a) can be estimated directly from the difference between the energy states and characterizes, whether a material is an insulator or semiconductor because of an existing band gap, a metal or semimetal because of band overlap or half-filled band. The number of charge carriers is responsible for the conductivity. Bands with a local minimum collect electrons in so-called electron pockets, which can be below or in the case of thermal excitement slightly above the Fermi energy. A hole pocket is a local maximum slightly above the Fermi energy. Doping of semiconductors changes the level of the Fermi-energy relative to the band structure, as occurring e.g. in PbTe.

For optical properties the type of excitement (Fig. 10b) is important. The direct interband transitions have a higher probability than the indirect transitions, because they require phonon scattering. When the extrema of the two bands are not at the same  $\underline{k}$ -vector, a so-called Burstein shift occurs: The excitement needs a higher energy than from the band gap expected. Bands with a smaller curvature in the  $E(k)$  diagram lead to higher effective carrier masses, which affect their mobility and hence the conductivity. In some cases bands with high or low effective masses overlap, so that intraband transitions are possible. Special features are observed in Na with its bcc-structure, which is almost like a free electron and hence a photon excitement with visible light (1-2 eV) is possible. In fcc-Cu an optical transition between a lower band and electron pockets is occurring, and this is one of the reason for its reddish color. In some semiconductors like Si or Ge two bands are almost parallel over a wide range of  $\underline{k}$ -vectors and this so-called tracking leads to a high dielectric constant.

Interpretation of the electron dispersion curves in three-dimensions (Fig. 10c), either as  $E(k_x, k_y, k_z)$  or as iso-energy-lines in  $\underline{k}$ -space, leads to the construction of the Fermi-surface, which can be very complicated for multi-valent metals (Cu, Al) and explains anisotropy effects. Finally, coupling effects between electrons

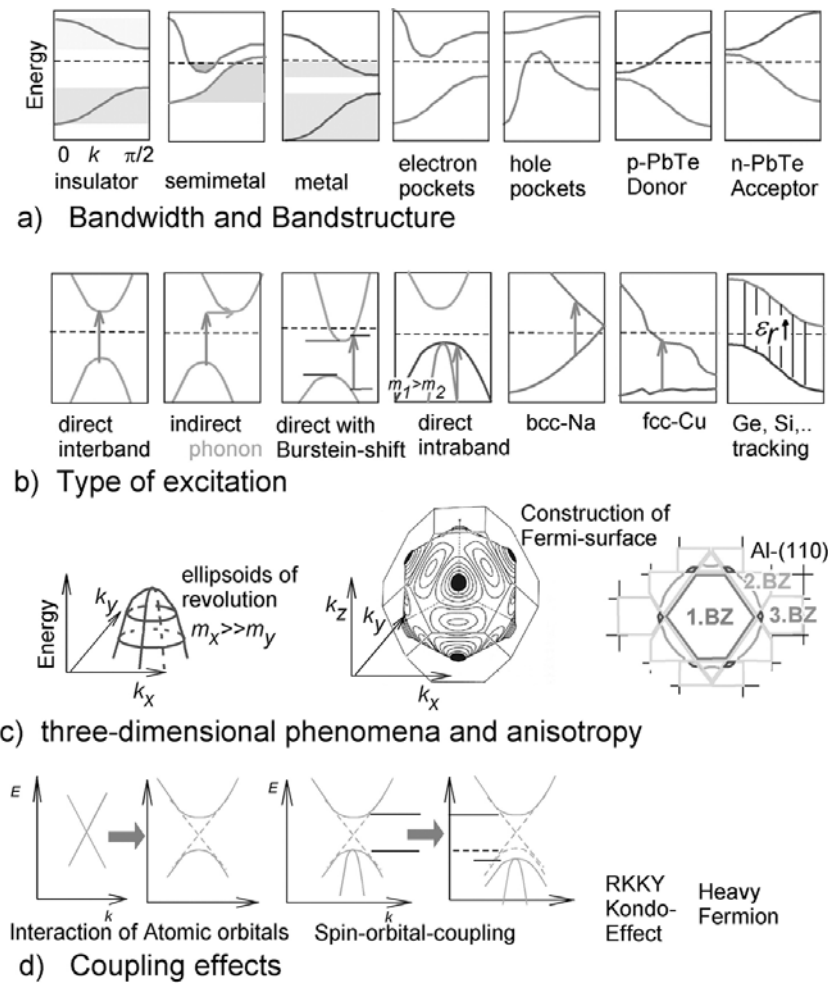


**Fig. 10.** Information obtained from electronic band structure calculations.

occur (Fig. 10d), which usually are not included in the conventional band-structure calculations based on the single-electron approximation. A common method is, to apply a post-calculation treatment on the band-structure, so that details like the interaction of atomic orbitals or the enlargement of the band-gap due to spin-orbital coupling appear in the final electron dispersion curve. However, strong coupling effects, like magnetic spin interaction (RKKY-effect), Kondo-effect, or heavy fermions are multi-electron effects in materials with d- and f-electrons are still lacking in understanding and numerical modeling.

## Discussion and Summary

This overview paper summarizes the needs for simulation, the calculation methods on different length scales, and the great facilities of *ab-initio* calculations. Numerical treatment of particles in liquids can be improved by the Voronoi method and especially the understanding of nano-particle agglomeration in a slurry and its prevention is the main goal for material simulation in future. Another challenge is, including effects of strong correlated electrons into the software. On the

other hand, many other questions in material science have been already solved and many new ideas for advanced materials came up by performing simulations. The modeling of nano-materials, surfaces, or interfaces requires a lot of creativity for building the supercells. Simulation cannot include all effects, and the researcher should be aware of the limitations, but it is worthwhile to start calculations from a certain point even for a restricted field of applications and so do innovative computational material science.

The experience has shown, that the most interesting materials science problems are the most difficult for calculations: Soft acoustic modes occurring in large systems, rotational modes of molecular units, or weak intermolecular forces in the presence of strong intramolecular forces, like the dynamic Van-der-Waals forces between ceramic particles, can take a long time until they converge during *ab-initio* calculations [41]. Also the present density functional theory, which is the base for the present *ab-initio* software, is limited to the one electron concept and hence, strong correlations are neglected, which would be necessary to improve for example calculations of thermoelectric materials. It is just a matter of time, computer development and the

number of simulation-software users, that such problems will be overcome in future.

### Acknowledgement

The author would like to thank Prof. Auh, Prof. Yong-Chae Chung (both Hanyang University), Prof. K. Niihara (Osaka University) for the invitation to write this paper, Prof. Masaki Tanemura (Nagoya Inst. Tech.) for help and patience, Prof. R. Podlucky, Prof. G. Kresse (both University Vienna), Prof. Deok-Soo Kim (Hanyang University), and Dr. Torsten Oekermann (Hannover University) for useful discussions.

### References

1. W. Wunderlich, and K. Niihara, *J. Ceramic Processing Res.* 4[1] (2003) 10-16.
2. K. Niihara, T. Sekino, T. Kusunose, and T. Nakayama, *Seramikkusu* 38[4] (2003) 255-263, *ibid.* 301-303.
3. W. Wunderlich, *Interceram* 51[3] (2002) 190-198.
4. Y. Masuda, W.S. Seo, and K. Koumoto, *Langmuir* 17 (2001) 4876-4880.
5. D. Schlettwein, T. Oekermann, T. Yoshida, M. Tochimoto, and H. Minoura, *J. Electroanal. Chem.* 481 (2000) 42-51.
6. T. Oekermann, D. Schlettwein, and N.I. Jaeger, *J. Phys. Chem. B* 105 (2001) 9524-9532.
7. T. Oekermann, T. Yoshida, D. Schlettwein, T. Sugihara, and H. Minoura, *Phys. Chem. Chem. Phys.* 3 (2001) 3387-3392.
8. I. Terasaki, Y. Sasago, and K. Uchinokura, *Phys. Rev. B* 56[20] (1997) R12685-R12687.
9. K. Takahata, Y. Iguchi, D. Tanaka, T. Itoh, and I. Terasaki, *Phys. Rev. B* 61[19] (15.05.2000) 12551-5.
10. Y. Ando, N. Miyamoto, K. Segawa, T. Kawata, and I. Terasaki, *Phys. Rev. B* 60 (1999) 10 580-3.
11. W. Koshibae, K. Tsutsui, and S. Maekawa, *Phys. Rev. B* 62[11] (15.09.2000) 6869-6872.
12. W. Shin, N. Murayama, and Z. Materials Letters 49 (2001) 262-266.
13. H. Sugawara, S. Osaki, S.R. Saha, Y. Aoki, H. Sato, Y. Inada, H. Shishido, R. Settai, Y. Ohnuki, H. Harima, and K. Oikawa, <http://arxiv.org/abs/cond-mat/0210601>.
14. S. Paschen, M. Baenitz, V.H. Tran, A. Rabis, F. Steglich, W. Carrillo-Cabrera, Y. Grin, A.M. Stydrom, and P.de V. du Plessis, *J. Phys. Chem. Sol.* 63 (2002) 1183-1188.
15. S. Paschen, W. Carrillo-Cabrera, A. Bentien, V.H. Tran, M. Baenitz, Y. Grin, and F. Steglich, *Physical Review B* 64[21] (2001) 214404-1-11.
16. S. Paschen, V. Pacheco, A. Bentien, A. Sanchez, W. Carrillo-Cabrera, M. Baenitz, B.B. Iversen, Y. Grin, and F. Steglich, *Physica B* 328 (2003) 39-43.
17. W. Wunderlich, K. Vishista, F.D. Gnanam, and D.D. Jayaleesan, *Proc. Int. Conf. Ceram. Processing Science ICCPS8*, Sep. 2002, Hamburg, Germany.
18. W. Wunderlich, D.D. Jayaseelan, and F.D. Gnanam, *Ceramic Soc. Japan, Autumn Meeting 14* (2001) 273-3K04.
19. A.A. Anappara, S.K. Ghosh, P.R.S. Warriar, K.G.K. Warriar, and W. Wunderlich, *Acta Materialia* 51 (2003) 3511-3519.
20. W. Wunderlich, P.N. Padmaja, and K.G.K. Warriar, *J. Europ. Ceramic Soc.* 24 (2004) 313-317.
21. D. Doni Jayaseelan, D. Amutha Rani, Tadahiro Nishikawa, Hideo Awaji, and F.D. Gnanam, *J. Eur. Ceram. Soc.* 20 (2000) 267-275.
22. J. Cordelair, and P. Greil, *J. Eur. Cer. Soc.* 20 (2000) 1947-1957.
23. J.S. Reed, *Principles of Ceramics Processing*, 2.Ed. John Wiley&Sons New York (1994).
24. R.J. Hunter, *Zeta-Potential in Colloid Science*, Academic Press New York (1981).
25. R.G. Horn, *J. Am. Ceram. Soc.* 73[5] (1990) 1117-1135.
26. J.A. Lewis, *J. Am. Ceram. Soc.* 83 (2000) 2341-59.
27. C.-W. Hong, *J. Am Ceram. Soc.* 80[10] (1997) 2517-24.
28. P. Greil, J. Cordelair, A. Betzhold, and Z. *Metallkde.* 92[7] (2001) 682-689.
29. W. Wunderlich, *Proc. 6th Eur. Conf. Rheology Erlangen*, Ed. H. Munstedt, J. Kaschta, A. Merten (2002) 277-8.
30. F. Mueller-Plathe, *Comput. Phys. Commun.* 78 (1993) 77-94, see also <http://www-theory.mpi-mainz.mpg.de/~mplathe/yasp.html> (April 2003).
31. F. Mueller Plathe, *Acta Polymer* 45 (1994) 259-293.
32. C. Bennemann, W. Paul, K. Binder, and B. Dunweg, *Physical Review E: Statistical Physics etc.* 57[1] (1998) 843-851.
33. S. Morooka, S. Zhang, T. Nishikawa, and H. Awaji, *J. Cer. Soc. Jpn.* 107[12] (1999) 1225-8.
34. K. Refson, *Physica B* 131 (1985) 256-266.
35. W. Wunderlich, and H. Awaji, *Proc. Int. Conf. Solid-Solid Phase Transf. '99 (JIMIC-3)*, Ed. by M. Koiwa, K. Otsuka, T. Miyazaki, The Japan Inst. of Metals, ISBN4-88903-401-3 3057 (1999) 781-783.
36. W. Wunderlich, and M. Takahashi, in: "Improved Ceramics through new Measurements, Processing, and Standards", *Ceramic Transactions Vol. 133*, Ed. M. Matsui, et al., *Am. Ceram. Soc.* (2002) 189-194.
37. W. Wunderlich, and H. Awaji, *Jour. Mat. Design* 22[10] (2000) 53-59.
38. A. Milchev, A. Milchev, and K. Binder, *Computer Physics Communications* 146[1] (2002) 38-53.
39. C.M. Fang, G.de With, and S.C. Parker, *J. Am. Cer. Soc.* 84[7] (2001) 1553-58.
40. D.-S. Kim, Y.-C. Chung, J.J. Kim, D. Kim, and K. Yu, *J. Ceramic Processing Res.* 3[3, II] (2002) 150-152.
41. Vasp tutorial course <http://cms.mpi.univie.ac.at/vasp-workshop>.
42. G. Kresse, and J. Hafner, *Phys. Rev. B* 47 (1993) 558, *ibid* 49 (1994) 14251.
43. G. Kresse, and J. Furthmueller, *Phys. Rev. B* 54 (1996) 11169.
44. Vasp Manual <http://cms.mpi.univie.ac.at/vasp>.
45. Vasp commercial version <http://www.materialsdesign.com/Pages/VASP.htm>.
46. N.H. de Leeuw, J.A. Purton, S.C. Parker, G.W. Watson, and G. Kresse, *Surface Science* 452[1-3] (2000) 9-19.
47. S.P. Bates, G. Kresse, and M.J. Gillan, *Surface Science* 385 (1997) 386-394.
48. S.P. Bates, G. Kresse, and M.J. Gillan, *Surface Science* 409[2] (1998) 336-349.
49. J.D. Chai, D. Stroud, J. Hafner, and G. Kresse, *Physical Review B: Condensed Matter and Materials Physics* 67[10] (2003) 104205.
50. S.G. Steinemann, W. Wolf, and R. Podlucky, *Color of intermetallic compounds*, in: *Intermetallic compounds Vol 3*, ed by J.H. Westbrook, R.L. Fleischer, Wiley Ch. Verlag Weinheim 2001.
51. Robert Arnold, *Stabilizing Pseudo-gap and scattering concept for non-crystalline materials*, Dissertation TU

- Chemnitz 1998, <http://archiv.tu-chemnitz.de/pub/1998/0005>.
52. M.S. Dresselhaus, Lecture on Solid-State Physics, 1. Review of Energy Dispersion Relations in Solids, MIT Boston 2001, [http://web.mit.edu/afs/athena/course/6/6.732/www/new\\_part1.pdf](http://web.mit.edu/afs/athena/course/6/6.732/www/new_part1.pdf) (April 2003).
53. W.A. Harrison, Electronic structure and properties of solids, Dover Pub. New York, 1989.
54. P.K. Basu, Theory of optical processes in Semiconductors, Claderon Press Oxford, 1997.